

THE EFFECT OF CONVENTIONAL INSTRUMENT TRANSFORMER TRANSIENTS ON NUMERICAL RELAY ELEMENTS

Demetrios Tziouvaras,
Jeff Roberts, Gabriel Benmouyal, and Daqing Hou
Schweitzer Engineering Laboratories
Pullman, WA USA

SUMMARY

Current and voltage transducers provide instrument level signals to protective relays. Protective relay accuracy and performance are directly related to the steady state and transient performance of the instrument transformers. Protective relays are designed to operate in a shorter time than the time period of the transient disturbance during a system fault. Large instrument transformer transient errors may delay or prevent relay operation. In this paper, we describe the effect of conventional instrument transformer transients on numerical relay elements and discuss numerical relay designs that cope with conventional instrument transformer transients. The elements we examine include distance, line differential, and breaker failure.

Current Transformer (CT) Transients

CT output is impacted drastically when the CT operates in the nonlinear region of its excitation characteristic [1]. Operation in this region is initiated by:

- Large asymmetrical primary fault currents with a decaying dc component.
- Residual magnetism left in the core from an earlier asymmetrical fault, or field-testing, if the CT has not been demagnetized properly.
- Large connected burden combined with high magnitudes of primary fault currents.

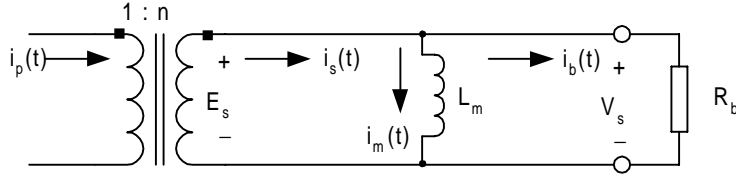
When the CT saturates because of the dc component, it can do so in the first few cycles of the fault. Long dc time constant offset faults can cause CTs to saturate many cycles after a fault. The fidelity of the transformation is reasonably good until saturation takes place. High-speed distance or instantaneous overcurrent relays may operate before CT saturation occurs.

Equation 1 gives the instantaneous CT secondary current, $i_s(t)$, as the sum of the instantaneous burden, $i_b(t)$, and the magnetizing, $i_m(t)$, currents.

$$i_s(t) = i_m(t) + i_b(t) \quad (1)$$

The CT steady-state magnetizing current is very small, as long as the CT operates in its linear region. If we assume that the exciting current is negligible, then the burden current, $i_b(t)$, is a replica of the primary current adjusted by the CT ratio. When the CT is forced to operate in its nonlinear region, the magnetizing current can be very large due to a significant reduction of the saturable magnetizing inductance value. The magnetizing current, which can be considered as an error current, subtracts from $i_s(t)$ and drastically affects the current seen by the connected burden on the CT secondary winding.

Figure 1 shows a simplified equivalent circuit of a CT that can be used for a simplified transient analysis.



$i_p(t)$ = primary current [A] V_s = CT secondary voltage output [V]
 E_s = CT secondary ideal voltage [V] R_b = connected burden resistance [Ω]
 L_m = magnetizing inductance [H]

Figure 1 Simplified CT equivalent circuit

We derived Equation 2 by solving Equation 1 for $i_m(t)$ with the following two assumptions:

- the CT is operating in the linear region below the knee point, and
- the CT time constant, $L_m/R_b = T_{CT}$, is very large.

$$i_m(t) = -\frac{I_p}{n} \left\{ \left(\frac{1}{\omega T_{CT}} \right) \sin \alpha - \left(\frac{T_s}{T_s - T_{CT}} \right) \left(e^{-t/T_s} - e^{-t/T_{CT}} \right) \right\} \quad (2)$$

where:

I_p = peak, symmetrical primary short circuit current

n = CT turns ratio

T_s = primary circuit time constant, $T_s = L/R$

L = power system inductance to the point of the fault

R = power system resistance to the point of the fault

Equation 2 shows that the transient magnetizing current consists of a steady-state and a transient term. The form of the transient term is the difference between two exponential terms, the same initial value but with two different time constants. One time constant equals that of the primary system, and the other equals that of the CT. The CT time constant typically is much longer than the primary system time constant, which implies that the transient conditions in the CT core persist after the dc primary transient disappears. In fact, when the primary current goes to zero due to breaker pole opening, a unipolar decaying current still flows in the secondary winding of the CT.

Relay Element Performance

Distance Relay (21) Elements

Digital mho type 21 element operating and polarizing vector quantities have been implemented as [2]:

$$S_{OP} = r \cdot ZI \cdot I_R - V_R$$

$$S_{POL} = V_{POL}$$

V_R and I_R are the voltage and current particular to an impedance loop (6 loops detect all faults), $Z1$ is the positive-sequence line impedance, r is the per-unit mho element reach (0.8 means 80 percent of the line), and V_{POL} is the polarizing voltage, consisting of the memorized positive sequence phasor [2]. A relay detects the fault as inside the mho element with reach when the scalar product between the two vectors is positive (i.e., the angle difference between S_{OP} and S_{POL} is less than 90 degrees) or:

$$\text{real}((r \cdot Z1 \cdot I_R - V_R) \cdot V_{POL}^*) \geq 0 \quad (3)$$

For a forward fault, this is equivalent to the reach, r , being greater than a distance, m , computed as in Equation 4:

$$r \geq m = \frac{\text{real}(V_R \cdot V_{POL}^*)}{\text{real}(Z1 \cdot I_R \cdot V_{POL}^*)} \quad (4)$$

If CT saturation occurs in one of the currents involved in the impedance loop, how is the computation of the inequality in Equation 4 impacted? I_R appears in the denominator of the calculated distance, m . During saturation, the magnitude of I_R reduces, and m has a higher value than ideal. From this, we can infer that a mho element underreaches during CT saturation.

Consider an A-phase fault on a 500 kV line ($Z1=75\angle 86^\circ$, $Z0=300\angle 75^\circ$). The fault occurs at 0.1 s at a distance from the relay equal to 33 percent of the line length.

As shown in Figure 3, m corresponding to a normal fault current settles to a value 0.33 as expected. For a saturated A-phase current (solid line in Figure 2), the calculated distance m value crosses the unity line with a half-cycle delay and settles around 0.45 because the current remains in a saturated state.

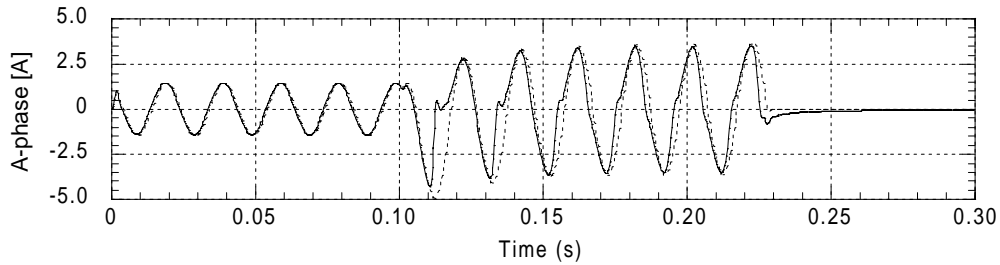


Figure 2 Saturated (solid) and normal (dashed) currents

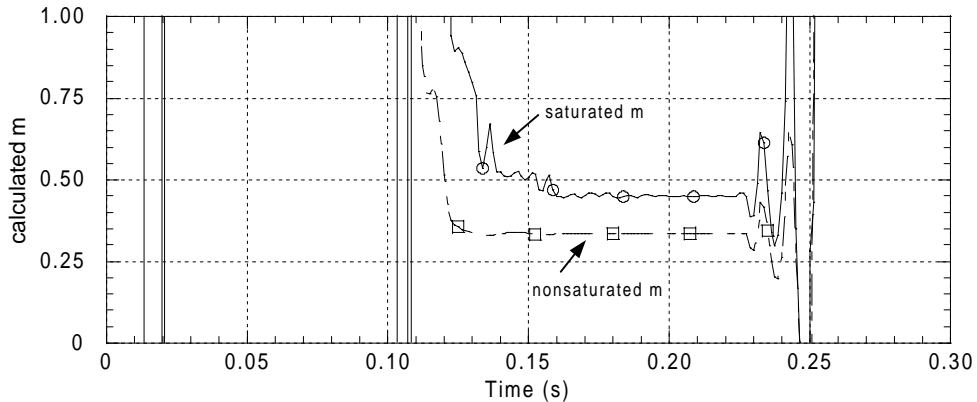


Figure 3 Calculated distances m values with normal and saturated currents

Figure 4 shows another method of visualizing distance relay element underreach because of CT saturation. Figure 4 shows the phasor diagram of the operating and polarizing vector quantities for a fault on the boundary of a self-polarizing mho distance element with reach r . As the CT saturates, the magnitude of I_R decreases, and its angle advances (this effect is shown as dashed lines in Figure 4). This causes the dV phasor to rotate counterclockwise which creates an element underreach.

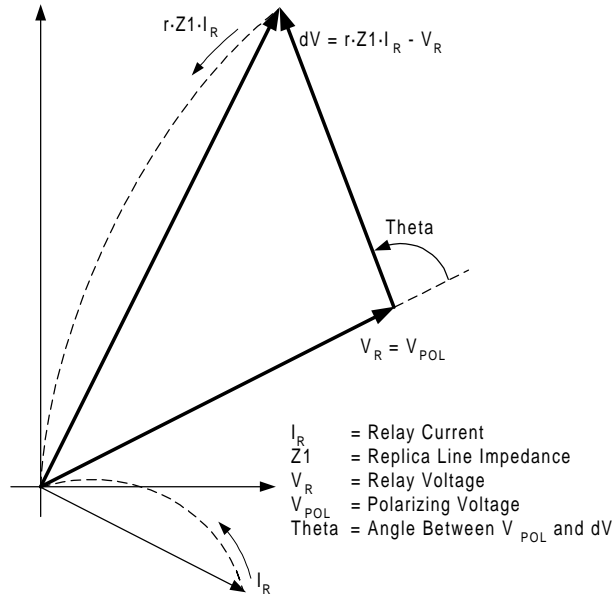


Figure 4 Mho element phasor diagram showing how CT saturation causes underreach

The possible impact of CT saturation on 21 elements is a minor delay of the corresponding Zone 1 element (assuming the CT does not remain in saturation because of the large current magnitude).

Zone 1 element underreach risk increases for fault locations near the relay reach. However, with moderate length lines, as the fault location approaches the relay reach, the fault current magnitude decreases to reduce the chances of CT saturation.

For larger reach Zone 2 or 3 elements, particularly in communication-assisted schemes (POTT, DCB, etc.), CT saturation has a limited impact on the final result, aside from a slight tripping delay.

Breaker Failure (BF) Relay Elements

Because BF operations affect many breakers, the speed with which a BF relay or scheme operates must be balanced with the need for secure breaker failure declarations. This balance is particularly important in Extra High Voltage (EHV) lines where stability of the power system is very critical. Therefore, BF relay overcurrent elements must display fast pickup and dropout times.

When the breaker interrupts the primary fault current, i.e., breaker poles open, the CT secondary output does not immediately go to zero current. Trapped magnetic energy in the CT exciting branch produces a unipolar decaying current with a fairly long time constant. In Figure 5 we see the unipolar decaying secondary current that still flows through the CT burden.

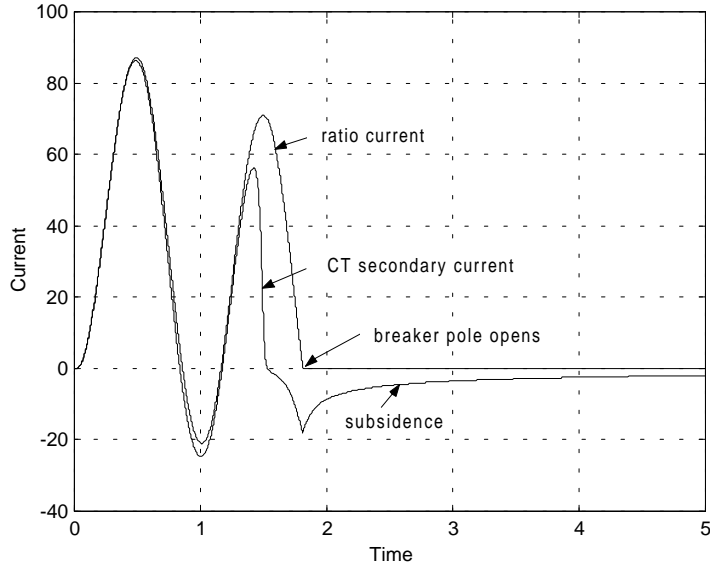


Figure 5 Subsidence current from a CT output after the breaker poles open

This unipolar decaying current, which is called subsidence current, can have a detrimental impact on BF relay operation that depends on resetting the BF scheme via fast overcurrent element dropout. The effect of the unipolar decaying current may be to create artificial phasor magnitudes that are large enough to prevent proper detection of the ac primary current interruption. This may delay the detection of BF overcurrent element dropout by some fraction of a cycle, and as a result, longer coordination intervals are needed in the BF logic to preserve scheme security.

Figure 6 compares the dropout time of a half-cycle cosine filter BF element (50FT) with that of an enhanced subsidence detection BF relay element (OPHA). Notice that the OPHA element asserts approximately 7 ms before the already rapid dropout 50FT element.

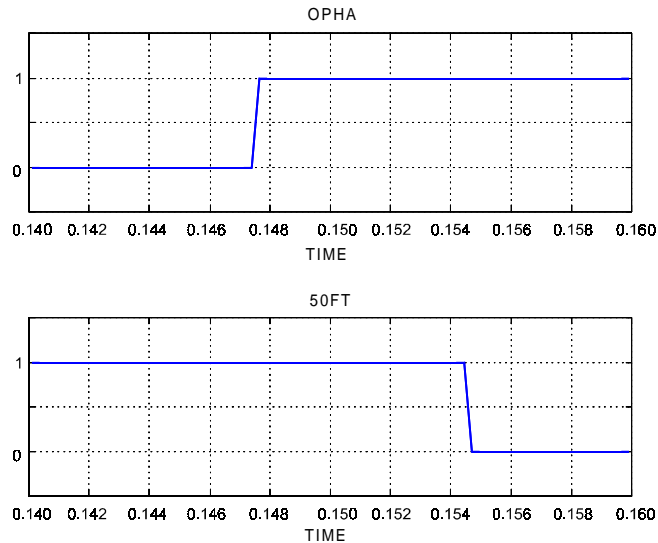


Figure 6 Half-cycle cosine filter (50BF) dropout and subsidence detection BF element (OPHA)

Breaker failure relay overcurrent elements must cope with this subsidence current. New microprocessor relays employ logic to detect the CT subsidence current, thereby speeding up the detection of overcurrent element dropout as shown by logic point OPHA in Figure 6.

Differential (87) Relay Elements

The plot in Figure 7 shows the results of two different yet secure line differential protection schemes for an out-of-section fault with CT saturation [3]. The complex plane shown is called the Alpha Plane. The cluster of points connected by a solid line represents the calculated ratio of I_R/I_L progressing in time with I_R being heavily saturated (I_R = remote relay current, I_L = local relay current). To obtain this figure, we calculated the fundamental phasor ratio of currents \vec{I}_L and \vec{I}_R from line-ends L and R, respectively.

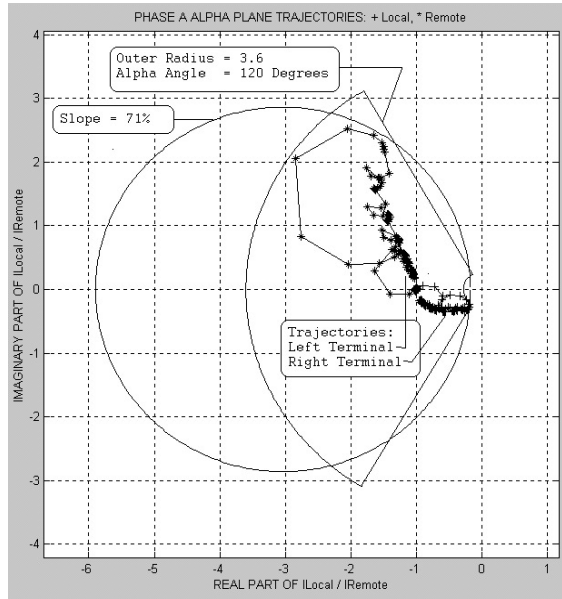


Figure 7 Alpha Plane plots of I_R/I_L , Alpha Plane Differential, and conventional differential characteristics

Both currents used are from 16 samples-per-cycle cosine filters. Without CT saturation the locus of the calculated ratio of I_R/I_L would be at the -1 point on the Alpha Plane, assuming negligible line-charging current. The circular characteristic shown is the representation of a slope characteristic on the Alpha Plane, corresponding to the conventional differential criterion:

$$|I_L + I_R| > K \cdot (|I_L| + |I_R|)$$

The slope value in the conventional differential relay is selected such that the relay characteristic encloses all the cluster of points where the difference current is above the minimum value. Notice that the Alpha Plane Differential element restraint region covers less area along the negative real axis than does the conventional slope methodology, yet both methods achieve the same security for CT saturation. The Alpha Plane Differential can sustain a very high level of external CT saturation by increasing both the radius, R , value and the angle, α , (up to 180 degrees) [3].

CAPACITOR VOLTAGE TRANSFORMER TRANSIENTS

Capacitor voltage transformers (CVTs) are widely used in high voltage power systems. Figure 8 shows a typical circuit diagram of a CVT. Capacitors C_1 and C_2 are used as a voltage divider to step down the line voltage before it is applied to a wound step down voltage transformer (SDT) via a tuning reactor L_{TR} .

Ferroresonance is a possibility in any system composed of capacitors and iron core inductances. In a CVT, the interaction of the source capacitance with the tuning reactor inductance and the SDT magnetizing inductance could lead to a ferroresonance oscillation.

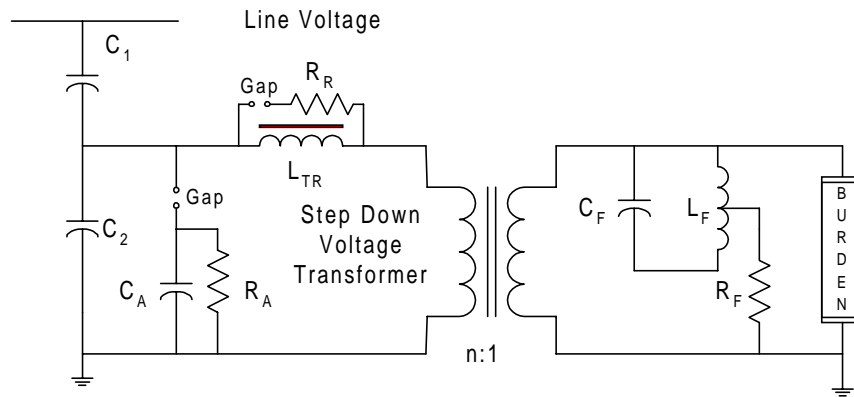


Figure 8 Capacitive voltage transformer circuit

CVT manufacturers use ferroresonance-suppression circuits (FSCs) to reduce or eliminate ferroresonance conditions. One such FSC device is shown connected at the secondary winding of the SDT in Figure 8. Capacitor C_F in parallel with L_F forms a high-impedance parallel resonant circuit tuned at the fundamental frequency. At harmonic or subharmonic frequencies, the FSC impedance drops off sharply leaving only the damping resistor, R_F , in the circuit. This is an active type of FSC. A passive FSC design uses passive elements to suppress the ferroresonance oscillations. The passive FSC design has a permanently connected resistor, R_F , in series with a saturable inductor, L_F , and an air-gap loading resistor. Under normal operating conditions, the secondary voltage is not high enough to flash the air gap and the loading resistor, R , has no effect on the CVT output.

Many CVT components and system conditions affect the CVT transient performance:

- High or extra high capacitance CVTs, higher STD ratios, and CVTs with passive FSCs display a better transient response.
- Small resistive burden, found in microprocessor relays, improves further the CVT transient response.
- Higher system impedance ratio (SIR) results in worse CVT transients for faults at the same location.
- Fault initiation angle influences the shape of CVT transients. The CVT transient is worse for faults at a voltage zero crossing.

Effect of CVT Transients on Distance Relay (21) Element Performance

CVT transients reduce the fundamental component of the fault voltage and cause distance relays to calculate a smaller than actual apparent impedance to the fault. Figure 9 shows the fundamental frequency magnitude of a CVT secondary voltage as compared with the ideal ratio voltage. Figure 10 shows two apparent impedance loci of an end-of-line fault calculated from the ideal ratio voltage and the CVT secondary voltage.

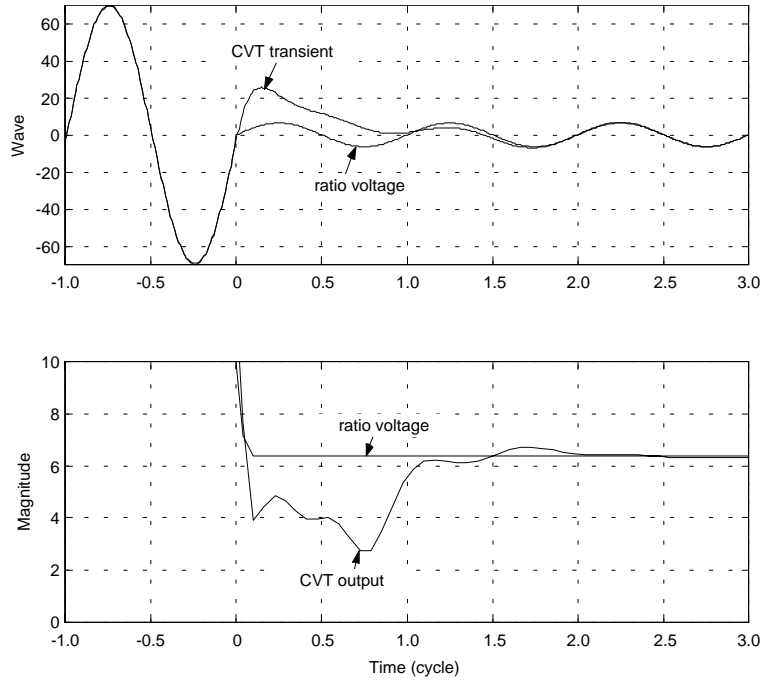


Figure 9 CVT transients reduce fundamental |V|

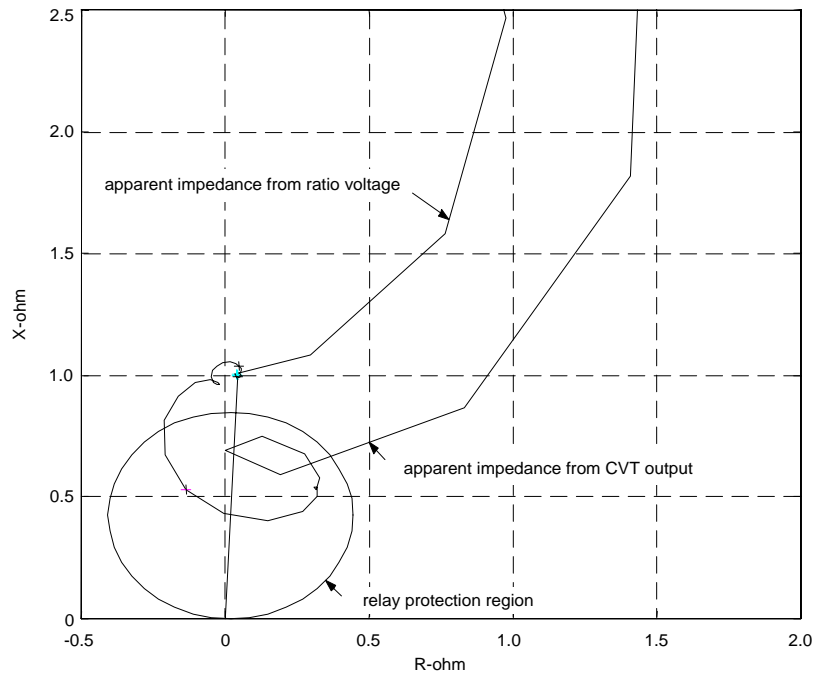


Figure 10 Overreach due to CVT transients

CVT Transient Detection Methods

Relay manufacturers have invented many solutions to cope with the CVT transient problem. These solutions include narrow band-pass filtering of the voltage (which effectively adds delay via filtering), reducing distance relay reach, and directly delaying the distance relay tripping

decision when a CVT transient condition is detected. All of these solutions have their inherent disadvantages. Reference [4] describes a patented solution that prevents distance relay CVT transient overreach. The logic detects high system impedance ratio (SIR) conditions that exhibit severe CVT transients and adds a time delay to the tripping decision. However, if the logic determines that the fault is close in, from the smoothness of the apparent fault impedance calculation, it overrides the time delay to permit rapid tripping for internal faults.

Figure 11 shows an end-of-line BC phase-to-phase fault. A Zone 1 instantaneous protection element is set at 85 percent of line length. The digital element plot shows that the Zone 1 element picks up because of the CVT transients but that the CVT transient detection logic successfully detects the overreach condition and blocks the Zone 1 element. This new logic overcomes the undesirable delay aspect by detecting when the CVT transient is complete and removes the Zone 1 element block.

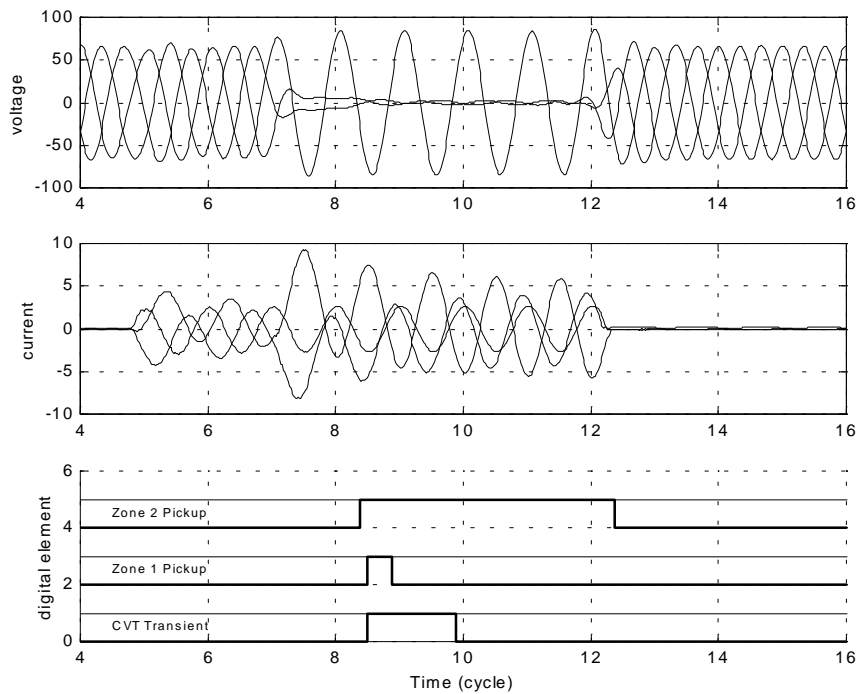


Figure 11 CVT transient detection logic prevents Zone 1 element from overreaching

CONCLUSIONS

In this paper we looked at how conventional instrument transformer transients affect numerical relay elements.

Distance relay Zone 1 elements exhibit a minor tripping delay, and a potential underreach for faults near the relay reach point, due to CT saturation. In general, faults near the relay reach point display a reduced current magnitude if the CT saturates. However, the chance of CT saturation near the relay reach point is much smaller than for faults occurring near the relay location. CT saturation has a limited impact, aside from a slight tripping delay, on longer set Zone 2 and Zone 3 distance elements.

CT subsidence current increases the dropout time of overcurrent relay elements used to detect breaker pole opening to reset BF schemes, unless they are fitted with CT subsidence detection logic.

CVT transients reduce the fundamental component of fault voltage and can cause overreach of Zone 1 distance relay elements. Relay elements fitted with CVT transient detection logic may introduce a slight (and necessary) tripping delay; however, they exhibit greater security for faults near the relay reach point.

Different differential relay element designs can cope with the same level of CT saturation, however, the Alpha Plane Differential element displays an increased sensitivity due to its design characteristic.

REFERENCES

- [1] Transient Response of Current Transformers, The Institute of Electrical & Electronic Engineers, Inc., New York, N. Y., January, 1976, 76 CH 1130-4 PWR.
- [2] E. O. Schweitzer III & J. Roberts, "Distance Relay Element Design," 19th Annual Western Protective Relay Conference, Spokane, Washington, USA, October 20–22, 1992.
- [3] J. Roberts, D. Tziouvaras, G. Benmouyal, and H. Altuve, "The Effect of Multi-Principle Line Protection on Dependability and Security," Southern African Power System Protection Conference, Johannesburg, South Africa, November 8–9, 2000.
- [4] D. Hou and J. Roberts, "Capacitive Voltage Transformers: Transient Overreach Concerns and Solutions for Distance Relaying," 22nd Annual Western Protective Relay Conference, Spokane, WA, USA, October 24–26, 1995.

BIOGRAPHIES

Demetrios A. Tziouvaras was born in Greece and moved to the USA in 1977. He received his B.S. and M.S. degrees in electrical engineering from the University of New Mexico and Santa Clara University, respectively. He joined the System Protection Group of Pacific Gas & Electric Company in 1980, where he held the position of Principal Engineer and was responsible for the application of new technologies, design standards, and substation automation. He joined Schweitzer Engineering Laboratories, Inc., as a Research Engineer in 1998. He is a senior member in the Institute of Electrical and Electronic Engineers (IEEE) and a member of the Power System Relaying Committee of the Power Engineering Society of IEEE. He is a member of two subcommittees and chairman of two working groups, one on EMTP Applications to Power System Protection and the other on Mathematical Models for Current, Voltage, and Coupling Capacitor Voltage Transformers. He has authored and co-authored numerous technical papers and taught seminars in EMTP, protective relaying, and digital relaying at the University of Illinois at Urbana-Champaign and the California Polytechnic Institute in San Luis Obispo, California. His interests include digital relay modeling, system protection, and power system transients. He holds one patent and has other patents pending.

Jeff Roberts received his B.S.E.E. from Washington State University in 1985. He worked for Pacific Gas & Electric Company as a Relay Protection Engineer for over three years. In 1988, he joined Schweitzer Engineering Laboratories, Inc., as an Application Engineer. He now serves as

Research Engineering Manager. He has delivered papers at the Western Protective Relay Conference, Texas A & M University, Georgia Tech, and the Southern African Power System Protection Conference. He holds multiple patents and has numerous patents pending. He is also a senior member of the IEEE.

Daqing Hou received B.S. and M.S. degrees in Electrical Engineering at the Northeast University, China, 1981 and 1984, respectively. He received his Ph.D. in Electrical and Computer Engineering at Washington State University in 1991. Since 1990, he has been with Schweitzer Engineering Laboratories, Inc., where he is currently a Research Engineer. His work includes system modeling, simulation, and signal processing for power system digital protective relays. His research interests include multivariable linear systems, system identification, and signal processing. He is a senior member of IEEE. He has multiple patents pending and has authored or co-authored several technical papers.

Gabriel Benmouyal received his B.A.Sc. in Electrical Engineering and his M.A.Sc. in Control Engineering from Ecole Polytechnique, Université de Montréal, Canada, in 1968 and 1970, respectively. In 1969 he joined Hydro-Québec as an instrumentation and control specialist. He worked on different projects in the field of substation control systems and dispatching centers. In 1978 he joined IREQ (Hydro-Québec research division) where his main field of activity was the application of microprocessors and digital techniques to substation and generating station control and protection systems. In 1997 he joined Schweitzer Engineering Laboratories, Inc., in the position of Research Engineer. He is a registered professional engineer in the Province of Québec, is an IEEE member, and has served on the Power System Relaying Committee since May 1989. He holds one patent and has several patents pending.